Progress In Electromagnetics Research Letters, Vol. 93, 115–122, 2020

Miniaturization of Microstrip Slot Antenna Using High Refractive Index Metamaterial Based on Single Ring Split Ring Resonator

G. Bharath Reddy*, M. Harish Adhithya, and D. Sriram Kumar

Abstract—In this paper, the miniaturization of the slot antenna is presented for the first time with the use of high refractive index metamaterial. Based on the effective parameter extraction, the studies conducted on Single Ring Split Ring Resonator (SR-SRR) reveal that the unit cell can produce high values of positive refractive index. By taking the advantage of the principle of duality, the slot is loaded with two Complementary SR-SRRs (CSR-SRRs) on either side of it to create an effective HRI medium. With the partial loading of HRI metamaterial medium, the resonance frequency of the slot is brought down from 4.225 GHz to 2.5 GHz. The radiation characteristics of the loaded slot antenna were found to be almost similar to that of the conventional slot antenna. The simulated and measurement results were found in good agreement.

1. INTRODUCTION

Portable wireless devices require wireless transceivers that are small. It is well known that antenna is the most space occupying component in an RF transceiver. So, reducing the size of the antenna is of prime interest of an RF designer. There are many techniques proposed for miniaturizing the antenna, among which the most common mechanism is reactance compensation [1]. Our main interest in this paper is slot antenna miniaturization. The reactance compensation was successfully applied by slit, strip, and loops to miniaturize a slot antenna [2–5]. The reactance compensation was applied by creating an effective ENG medium with array of wires [5]. Reactance compensation was successfully demonstrated for miniaturization of slot antennas by [2, 5]. The feasible use of the metamaterial DNG spherical shells around the antennas is demonstrated theoretically to increase the radiation efficiency of the electrically small antennas [6]. However, because of their anisotropy, it is known that implementing such a shell with metamaterials is impossible. Despite the difficulty of implementing isotropic DNG shells, an ENG shell with CSRR is introduced on a wire monopole antenna ground plane to decrease the resonance frequency [7]. It is also shown that zeroth order resonance can bring the miniaturization. However, still, [7] and [8] are narrow band techniques due to dispersion of effective parameters. The ability of the Epsilon Very Large (EVL) or Mu Very Large (MVL) medium to reduce size of the antenna is theoretically speculated in addition to realizing negative parameter media [9]. Nevertheless, metamaterials based on EVL or MVL have not been introduced or integrated for antenna miniaturization applications so far.

For the first time, with the studies conducted on the Single Ring Split Ring Resonator's effective medium abilities, it is discovered that it would be used as a metamaterial unit cell for the sake of manifesting the effectively high refractive index medium to miniaturize the wire monopole antenna in our previous work [10]. In this paper, miniaturization of the slot antenna is performed with loading of HRI metamaterial medium composed of CSRSRRs.

Received 6 June 2020, Accepted 17 September 2020, Scheduled 5 October 2020

* Corresponding author: Gudibandi Bharath Reddy (bharath09478@gmail.com).
The authors are with the Department of Electronics and communication Engineering, National Institute of Technology, Tiruchirappalli, India.

2. ANTENNA DESIGN

It is not enough to obtain EVL or MVL property itself to miniaturize an antenna. However, the combined impact of permittivity and permeability should result in an effectively high refractive index. The refractive index would also be a complex number, as permittivity and permeability are complex numbers, and the refractive index is also product of two such complex numbers. From the refractive index relation given below in Equation (2), it could be understood.

$$n = \sqrt{\mu\varepsilon} \quad \text{whereas,} \quad \mu = \mu' + j\mu'' \quad \text{and} \quad \varepsilon = \varepsilon' + j\varepsilon'' \tag{1}$$

From Equation (1), refractive index n can be written as,

$$n = \sqrt{(\mu'\varepsilon' - \mu''\varepsilon'') + j(\mu'\varepsilon'' + \mu''\varepsilon')} \tag{2}$$

In our investigation about the SR-SRR as shown in Fig. 1(a), the refractive index is found to be of high value just below its fundamental resonance frequency. The frequency of fundamental resonance would be identified from the transmission characteristics of the SR-SRR, i.e., 2.9 GHz as shown in Fig. 1(b)).

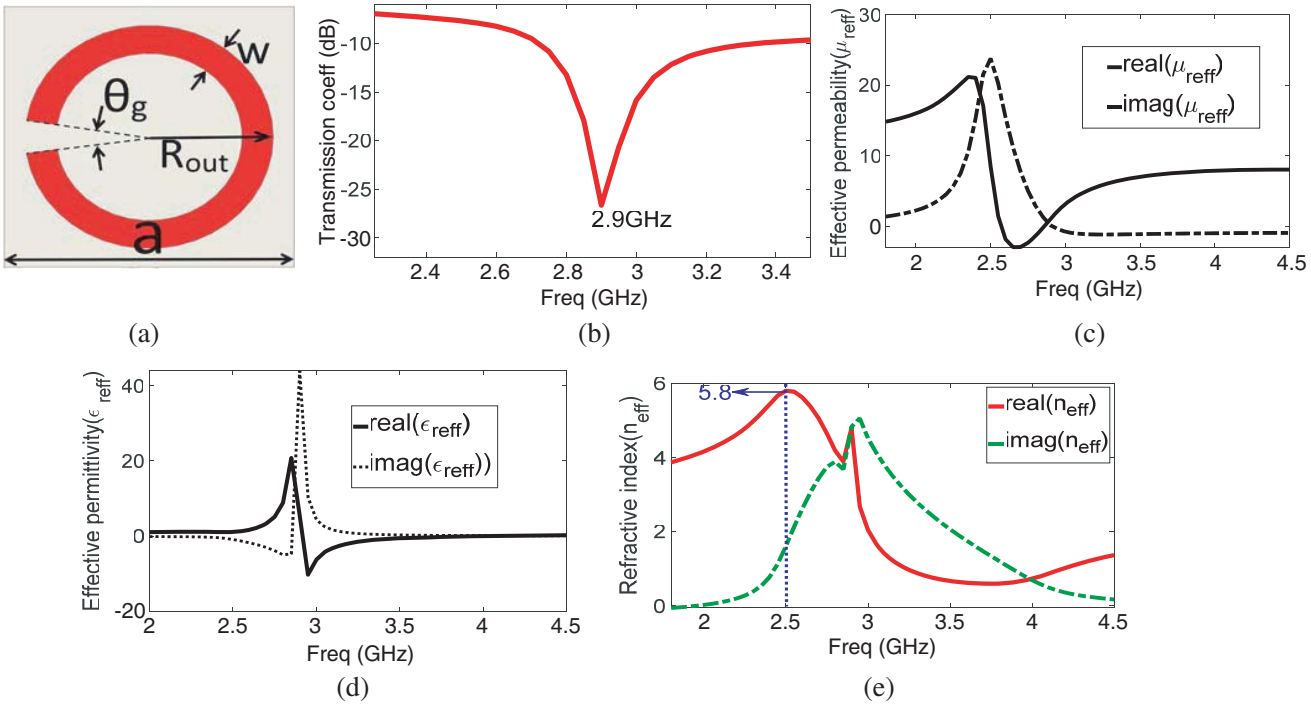

Figure 1. (a) SR-SRR unit cell with $R_{out} = 6\,\text{mm}$, $w = 4.5\,\text{mm}$, and $\theta_g = 17^\circ$ and $a = 14\,\text{mm}$. (b) Transmission coefficient of SR-SRR unit cell simulated HFSS, and the extracted effective medium parameters. (c) Permeability, (d) permittivity and (e) refractive index.

Approximate resonance frequency value for SR-SRR could be calculated using the equations given by [11]. Since the unit cell resonance frequency calculated from the analytical expressions is not accurate, the unit cell dimensions are varied to see the impact on the resonance frequency and the refractive index peak with fewer losses (less value of imaginary part of the refractive index). It could be seen from Fig. 1(c) that the extracted value of the permeability has a maximum at 2.5 GHz. Similar to the variation of permeability, the extracted value of the effective permittivity also has maximum at 2.85 GHz as shown in Fig. 1(d). Bearing in mind that the refractive index is a product of the permeability and permittivity, the achieved first peak in the refractive index at 2.5 GHz could be seen as a peak in the permeability plot at 2.5 GHz, and the second peak at 2.85 GHz could be seen as a peak in the permittivity plot at 2.85 GHz. For the dimensions of SR-SRR shown in Fig. 1(a), the first peak with a value of 5.8 (as shown in Fig. 1(e)) is achieved in the real part of the refractive index at 2.5 GHz and

the second peak with a value of 4.8. The second peak is not considered for the design of the antenna because of the high value of the imaginary part of refractive index.

With the help of the theory of duality [12], the permittivity and permeability of the CSR-SRR and SR-SRR could become dual of each other. That means $\mu_{eff_{SR\text{-}SRR}} = \varepsilon_{eff_{CSR\text{-}SRR}}$ and vice versa. The effective parameter extraction was carried out with the help of Krammer-Kronig based unique extraction procedure [13]. However, the extracted effective refractive index of the unit cell remains the same as it is a product of the permittivity and permeability. From the above argument, the effective refractive index of the CSR-SRR also follows the same variation shown in Fig. 1(e).

A CSR-SRR unit cell with the dimensions similar to that of SR-SRR as shown in Fig. 1(a) is considered for incorporation into the slot antenna as CSR-SRR. The CSR-SRR is preferred over SR-SRR because of the advantage that CSR-SRR does not need to use another side of the substrate as SR-SRR unit cell. It is well known that the electric field inside a slot at fundamental resonance follows the sinusoidal variation along the length and will be very high in the middle of the slot. In order to excite the CSR-SRR properly with the slot electric fields and to match magnetic currents along with maintaining symmetry in loading, two CSR-SRRs were etched on either side of the slot with an overlap as shown in Fig. 2.

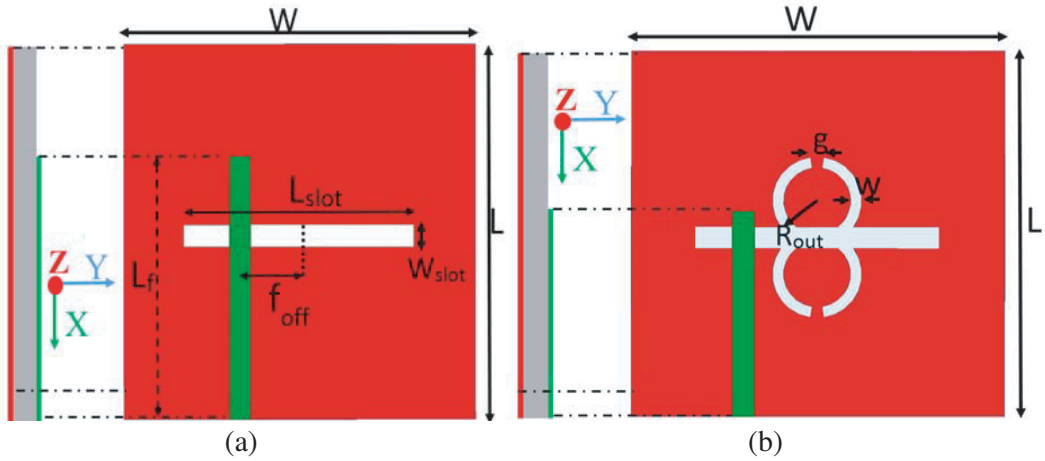

Figure 2. The 3D model of the proposed antenna structure. (a) Unloaded slot antenna. (b) CSR-SRR loaded slot antenna.

The topology of the slot antenna composed of a microstrip feed line and a slot in the middle of the ground plane on either side of the FR-4 substrate with $\varepsilon_r = 4.4$ as shown in Fig. 2. The width and length of the ground plane are $W = L = 60\,\text{mm}$. And the width and length of the slot are $W_{slot} = 3\,\text{mm}$ and $L_{slot} = 32.72\,\text{mm}$. Length of the slot is selected such that it will be half of the free space wave length at the resonance frequency (4.225 GHz). The CSR-SRRs were symmetrically loaded at the center of slot on either side of its length so that the loading should not affect the radiation pattern.

3. PARAMETRIC ANALYSIS

The introduction of two CSR-SRR unit cells on either side of the conventional slot antenna will change the impedance properties of the loaded antenna. The CSR-SRR unit cells would add additional reactance onto the slot and thus disturbs the conventional sinusoidal distribution of electric field. This will, in turn, change the variation of the impedance along the length of the slot. In order to match such a loaded slot, the microstrip feed line position and length need to be changed. For better impedance matching, parametric analysis of L_f (feed line length) and f_{off} (position relative to the centre of the slot) is carried out, which is shown in Fig. 3.

Initially, the value of f_{off} is varied to see the impact on the matching performance as shown in Fig. 3(a). It is observed that very good matching is obtained at $f_{off} = 11.5\,\text{mm}$ with the resonance frequency of 2.875 GHz which is near the second peak in the refractive index. By keeping f_{off} as a

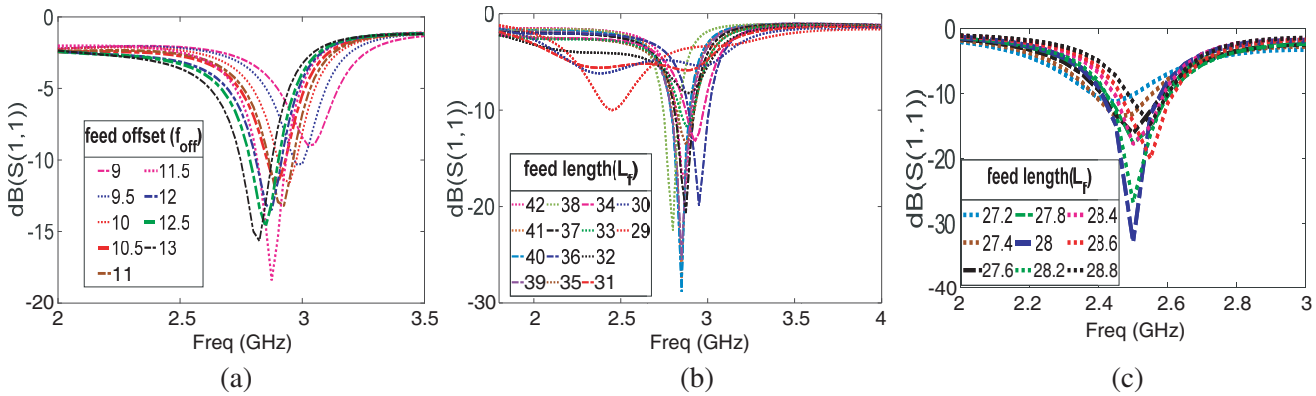

Figure 3. Input reflection coefficient variation with parametric variation of (a) feed offset foff (at Lf=35mm) and (b) feed length (at $f_{off} = 11.5$ mm) and (c) fine tuning of feed length. All the dimensions in the plot are in mm.

constant at 11.5 mm, the feed length (L_f) is varied to observe the effect on impedance matching as shown in Fig. 3(b). The value of L_f is varied from 29 mm to 42 mm over the slot. For all the values above 32 mm, the resonance near the frequency corresponding to the second peak in refractive index only got excited. However, at the lowest value of L_f which is 29 mm, it is found that a resonance near 2.5 GHz got excited. At the same time, a peak value of 5.8 in the refractive index variation is also observed at 2.5 GHz as shown in Fig. 1(e).

So, to study it further, parametric analysis is conducted again on the feed length L_f, for values less than 29 mm, which is shown in Fig. 3(c). This study shows that a deep resonance is excited at 2.5 GHz. As mentioned before, a peak refractive index of 5.8 is also obtained at 2.5 GHz for the metamaterial unit cell. Since the good impedance matching is achieved at 2.5 GHz for the values of $L_f = 28$ mm and $f_{off} = 11.5$ mm, the above-mentioned dimensions of L_f and f_{off} are finalized and applied to the proposed antenna shown in Fig. 2(b). The simulations were carried out using the High Frequency Structure Simulator (HFSS).

The lumped equivalent circuit model of the slot antenna is shown (in Fig. 4(a)) in order to further analyse the loading of the CSR-SRR. Here, R_{sh} is the shunt resistance, and L_{sh}, C_{sh} are shunt inductance and shunt capacitances, respectively. The LC resonant circuit shown in Fig. 4(b) represents the CSR-SRR unit cell. Here, L_R and C_R are the equivalent inductance and capacitance of the ring resonator CSR-SRR. The values of L_R and C_R are calculated using the equations mentioned in [11], and they are found to be $L_R = 15.3$ nH and $C_R = 0.14$ pF, respectively. As the CSR-SRR and slot antenna are electromagnetically coupled, the coupling between them is represented with M. By using the genetic algorithm-based optimisation technique in the Keysight Advanced Design System (ADS) commercial package with keeping the L_R and C_R values as mentioned above, appropriate values of the circuit parameters have been found. They are $L_{sh} = 0.1$ nH, $C_{sh} = 40.12$ pF, $R_{sh} = 49.63\,\Omega$, respectively. It is also found that the impedance matching performance of the circuit-based simulation and full wave simulation are in agreement. It is plotted in the Fig. 4(d). For the easier understanding, the equivalent circuit in Fig. 4(b) is modified to a new form (Fig. 4(c)) where L_R and C_R were transformed to L'_R and C'_R. From Figs. 4(b) and 4(c), it could be understood that L'_R will be in series with L_{sh} after the transformation, thus the total effective inductance value increases and results in the decrease in the value of resonance frequency of the antenna. The increment in the inductance after loading can also be attributed to the increased value of effective permeability around the antenna which can be referred to as High effective Refractive index (as the refractive index is nothing but the product of the permeability and permittivity).

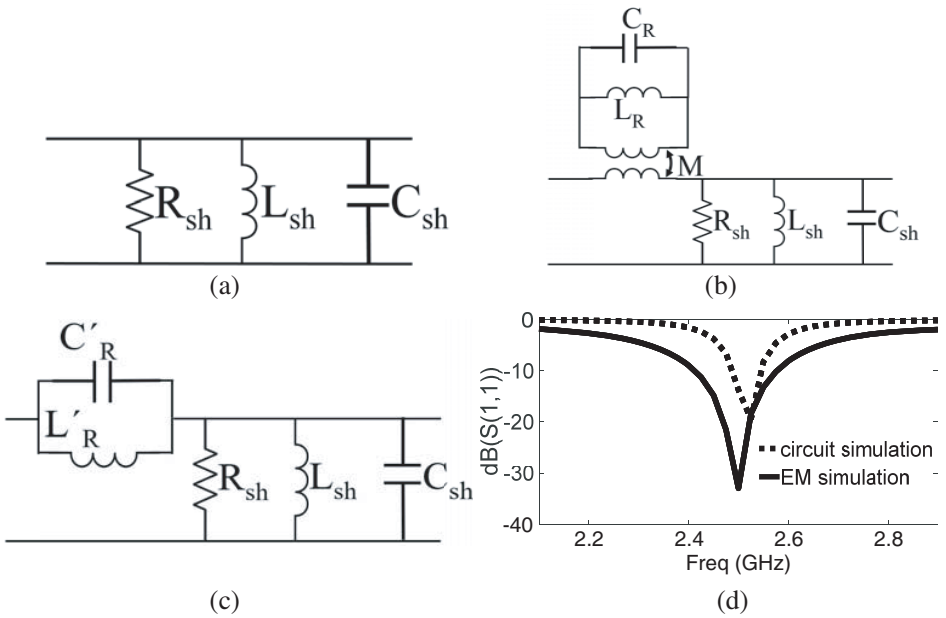

Figure 4. Transmission line equivalent circuit of (a) slot antenna, (b) CSR-SRR loaded slot antenna, (c) after applying impedance transformation to (b) and (d) input reflection coefficient comparison of circuit simulation and EM simulation.

4. RESULTS AND DISCUSSION

Figure 5(a) indicates the reflection coefficient plot of loaded and unloaded slot antennas. It is noted that the unloaded slot antenna resonates at 4.225 GHz which is its fundamental resonance. This is verified by the distribution of magnetic current shown in the Fig. 5(b). The slot antenna loaded with HRI medium composed of two CSR-SRRs resonates at 2.5 GHz. With the HRI medium loading, the standing wave length shrinks through the existence of the HRI medium which could be seen in Fig. 5(c). Here, the HRI metamaterial medium is essentially used to squeeze the large wave length in a small space. It is also noted from Fig. 5(c) that in the field of impact of the efficient HRI medium there is a sudden sinusoidal variation in the magnetic current. The field of impact of the HRI medium is tiny and does not cover the entire room of the antenna. It reduces the resonance frequency from 4.225 GHz to 2.5 GHz with its lower efficient presence of about 1/6th of the room, which is about 41% decrease in the resonance frequency.

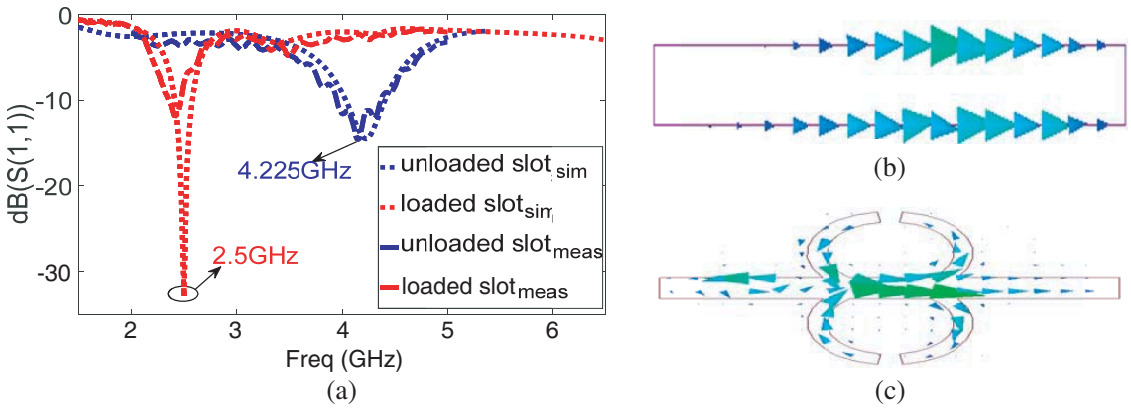

Figure 5. (a) The S_{11} variation with frequency for different versions of slot antenna. (b) Magnetic current distribution in unloaded slot at 4.225 GHz and (c) in HRI medium loaded slot at 2.5 GHz.

The simulated radiation patterns of the loaded and unloaded slot antennas are displayed in Fig. 6. The radiation pattern of the loaded antenna at the reduced resonance frequency should be comparable to that of the unloaded resonance to demonstrate the resonance at 2.5 GHz owing to the HRI metamaterial operation. It is confirmed that the radiation pattern of the HRI medium loaded slot antenna is still omnidirectional in the E-plane (in Fig. 6(a)) and figure of eight in the H-plane (in Fig. 6(b)) which is similar to that of the conventional slot antenna's fundamental resonance. From the radiation patterns shown in Fig. 6, it is identified that the slot is still operating in its fundamental mode of resonance after loading.

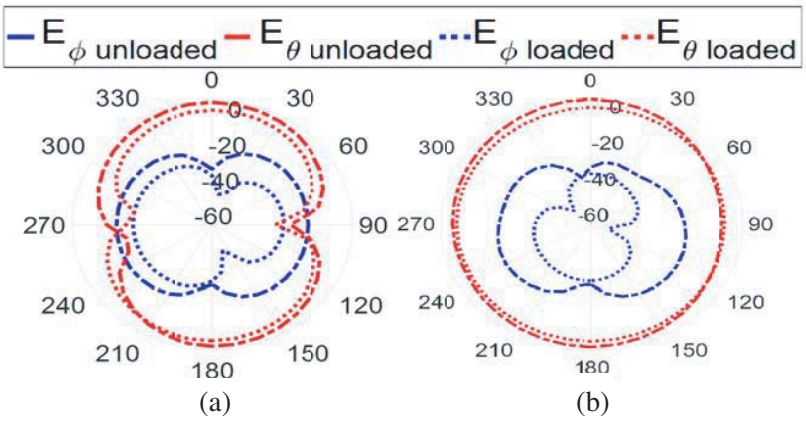

Figure 6. (a) The H-plane and (b) E-plane simulated patterns of unloaded slot at 4.225 GHz and loaded slot at 2.5 GHz.

The loaded slot antenna's measured radiation patterns are shown in Fig. 7. The radiation patterns of measured and simulated are discovered to be very comparable. The variation of the simulated results in the H-plane and E-plane nearly agrees with that of the measured results. It can be believed that the mechanism of HRI metamaterial works well in miniaturization based on the following argument from the understanding of the mentioned results.

1. The phenomena can be explained by metamaterials because the magnetic current distribution (as shown in Fig. 5(b)) within the slot with the help of the simulations is shrink within the smaller space because of the higher refractive index created by the loading of CSRSRRs.
2. Also, the similarity in the radiation patterns of the loaded and unloaded antennas would further reinforce this argument (From Fig. 6 and Fig. 7), because the presence of HRI medium around the antenna would not alter the shape of the antenna but decreases the resonance frequency only.

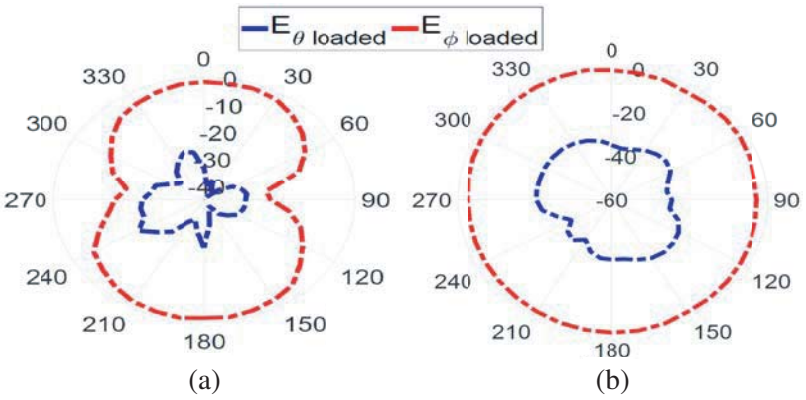

Figure 7. (a) The H-plane and (b) the E-plane measured patterns of loaded slot at 2.5 GHz.

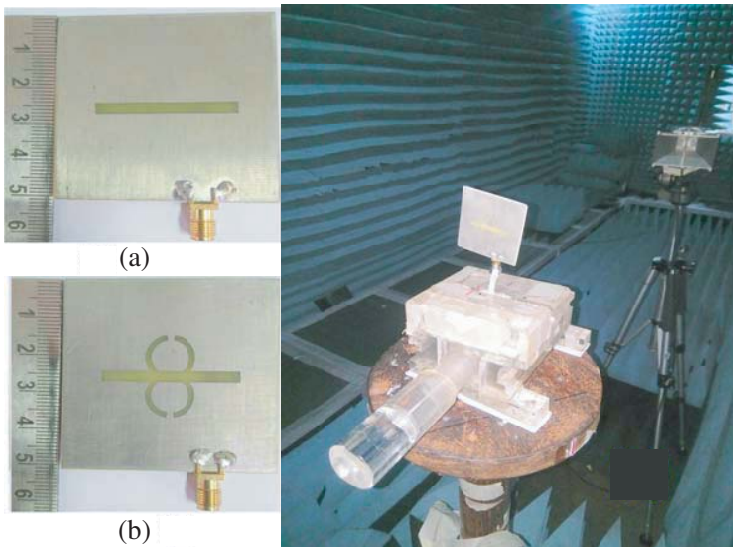

Figure 8. Fabricated prototypes of the antennas. (a) Unloaded slot, (b) loaded slot and (c) antenna during measurement in anechoic chamber.

From the above two points, the lack of a periodic structure of the large number of unit cells to produce the homogeneous HRI effective medium can be overlooked. As the electric/polarizability does not change with the number of unit cells, even with a smaller number of unit cells a similar kind of effective medium can be formed. The fabricated prototypes are shown in Fig. 8(a) and Fig. 8(b). The fabricated antennas are evaluated in an anechoic chamber for radiation patterns as shown in Fig. 8(c). And the fabricated antennas are tested with Agilent 5062A ENA. The HRI medium loaded slot antenna's measured gain is -1.1 dB while the standard unloaded slot antenna's gain is 1.95 dB. The gain decrease would be due to the loss connected with the refractive index's imaginary portion. Table 1 presents the comparison between the literature and our technique. It can be observed that the present technique made a good attempt in miniaturizing the antenna with almost 40.8% of miniaturization. In our previous work, the HRI medium was used on a non-planar antenna whereas it is used on a planar antenna in the present work.

Table 1. Comparison with the existing literature.

Ref.	Size in λ^3	Type of loading	Gain	Miniaturization (%)
[2]	$0.8 \times 0.8 \times 0.02$	Loop	-3.4 dB	26.01
[3]	$1 \times 1 \times 0.015$	Slit and strip	0.5 dB	37.73
[4]	$0.96 \times 0.96 \times 0.02$	Wire (ENG)	2.3 dB	28.83
[5]	$3.93 \times 3.93 \times 0.01$	Loop, slit, strip	NA	48.01
[7]	$0.27 \times 0.27 \times 0.115$	ENG loading	3.48 dB	55.3
[8]	$0.33 \times 0.33 \times 0.02$	CRLH ZOR	5.72 dB	NA
Previous work [10]	$0.41 \times 0.41 \times 0.13$	HRI metamaterial	-1.4 dB	45.7
Present work	$0.5 \times 0.5 \times 0.01$	HRI metamaterial	-1.1 dB	40.8

5. CONCLUSION

In this paper, with the help of CSR-SRR, a large value of the refractive index is shown to be achieved. With the assistance of parametric extraction, the capacity to produce elevated refractive index from

SR-SRR is described. By loading the conventional slot antenna with an HRI metamaterial medium, 41% reduction in the resonance frequency is achieved without degradation in the shape of radiation pattern. In the future, loading it onto other kinds of antennas for distinct applications will further investigate the same unit cell.

ACKNOWLEDGMENT

This work is supported by the Ministry of Electronics and Information Technology (MietY) under the Visweswarayya PhD scheme with grant No. Phd-MLA- 4(16)/2015-16. The author would like to thank Mr. Dushyanth Marathe from NIT, Nagpur for his useful discussions and suggestions. The author also wants to thank Prof. K. Vasudevan for providing the testing facility for pattern measurements.

REFERENCES

1. Fallahpour, M. and R. Zoughi, "Antenna miniaturization techniques: A review of topology- and material-based methods," *IEEE Antennas and Propagation Magazine*, Vol. 60, No. 1, 38–50, Feb. 2018.
2. Ghosh, B., S. M. Haque, D. Mitra, and S. Ghosh, "A loop loading technique for the miniaturization of non-planar and planar antennas," *IEEE Transactions on Antennas and Propagation*, Vol. 58, No. 6, 2116–2121, Jun. 2010.
3. Ghosh, B., S. M. Haque, and D. Mitra, "Miniaturization of slot antennas using slit and strip loading," *IEEE Transactions on Antennas and Propagation*, Vol. 59, No. 10, 3922–3927, Oct. 2011.
4. Haque, S. M. and K. M. Parvez, "Slot antenna miniaturization using slit, strip, and loop loading techniques," *IEEE Transactions on Antennas and Propagation*, Vol. 65, No. 5, 2215–2221, May 2017.
5. Ghosh, B., S. K. M. Haque, and N. R. Yenduri, "Miniaturization of slot antennas using wire loading," *IEEE Antennas and Wireless Propagation Letters*, Vol. 12, 488–491, 2013.
6. Ziolkowski, R. W. and A. D. Kipple, "Application of double negative materials to increase the power radiated by electrically small antennas," *IEEE Transactions on Antennas and Propagation*, Vol. 51, No. 10, 2626–2640, Oct. 2003.
7. Tang, M. and R. W. Ziolkowski, "A study of low-profile, broadside radiation, efficient, electrically small antennas based on complementary split ring resonators," *IEEE Transactions on Antennas and Propagation*, Vol. 61, No. 9, 4419–4430, Sept. 2013.
8. Lai, A., K. M. K. H. Leong, and T. Itoh, "Infinite wavelength resonant antennas with monopolar radiation pattern based on periodic structures," *IEEE Transactions on Antennas and Propagation*, Vol. 55, No. 3, 868–876, Mar. 2007.
9. Lovat, G., P. Burghignoli, F. Capolino, and D. R. Jackson, "Combinations of low/high permittivity and/or permeability substrates for highly directive planar metamaterial antennas," *IET Microwaves, Antennas & Propagation*, Vol. 1, No. 1, 177–183, Feb. 2007.
10. Bharath Reddy, G., M. Harish Adhithya, and D. Sriram Kumar, "Miniaturization of monopole antenna using high refractive index metamaterial loading," *International Journal of RF and Microwave Computer Aided Engineering*, e22163, 2020.
11. Jabita, A. A., "Design of singly split single ring resonator for measurement of dielectric constant of materials using resonant method," Univ. of Gavle, 2013.
12. Getsinger, W. J., "Circuit duals on planar transmission media," *IEEE MTT-S International Microwave Symposium Digest*, 154–156, Boston, MA, USA, 1983.
13. Szabo, Z., G. Park, R. Hedge, and E. Li, "A unique extraction of metamaterial parameters based on Kramers-Kronig relationship," *IEEE Transactions on Microwave Theory and Techniques*, Vol. 58, No. 10, 2646–2653, Oct. 2010.